Available online at www.sciencedirect.com

ScienceDirect

Energy Procedia 77 (2015) 296 – 303

Energy Procedia

5th International Conference on Silicon Photovoltaics, SiliconPV 2015

# TCO-free low-temperature $p^+$ emitters for back-junction c-Si solar cells

Isidro Martín[a,]*, Arnau Coll[a], Gema López[a], Pablo R. Ortega[a], Thibaut Desrues[b], Albert Orpella[a], Ramón Alcubilla[a]

[a] *Departament d'Enginyeria Electrònica, Universitat Politècnica de Catalunya, C/Jordi Girona 1-3, Mòdul C4, 08034 Barcelona, Spain*
[b] *INES-CEA, 50 Avenue du Lac Léman, BP 332, 73370 Le Bourget du Lac, France.*

**Abstract**

In this work, we report on the fabrication and characterization of n-type c-Si solar cells whose $p^+$ emitters are based on laser processed aluminum oxide/silicon carbide ($Al_2O_3/SiC_x$) films. The $p^+$ emitter is defined at the rear side of the cell and it consists of point-like laser-diffused $p^+$ regions with a surface charge induced emitter in between based on the high negative charge located at the $Al_2O_3$/c-Si interface. These emitters are fabricated at low temperature (< 400 ºC) and could be directly compared to silicon heterojunction emitters with the advantage that the deposition of a Transparent Conductive Oxide (TCO) film can be avoided, since they are based on $p^+$/n c-Si homojunctions. Additionally, the involved films are transparent to the IR photons (□ >1000 nm) that reach the rear surface of the cell resulting in an excellent back reflector. We fabricated solar cells with distance between $p^+$ regions or pitch ranging from 200 to 350 µm with a front surface based on silicon heterojunction technology. Best efficiency (18.1 %) is obtained for a pitch of 250 µm as a consequence of the trade-off between $V_{oc}$ and *FF* values.


Peer review by the scientific conference committee of SiliconPV 2015 under responsibility of PSE AG

*Keywords:* DopLa cell, laser doping, back-junction, c-Si solar cells

* Corresponding author. Tel.: +34-93-4054193; fax: :+34-93-4016756.
*E-mail address:* isidro.martin@upc.edu


Peer review by the scientific conference committee of SiliconPV 2015 under responsibility of PSE AG
doi:10.1016/j.egypro.2015.07.042

## 1. Introduction

In the last years, heterojunction silicon solar cells have been intensively developed based on the Heterojunction with Intrinsic Thin layer (HIT) concept with excellent results [1-2]. Among them, the results obtained by the combination of this technology with Interdigitated Back-Contacted (IBC) structures are particularly impressive [3-4]. The fabrication process of all these devices replaces the conventional high-temperature (800-900 ºC) thermal step for the diffusion of dopant impurities by a low temperature (200-250 ºC) deposition of amorphous silicon (a-Si:H) films resulting in a cost effective fabrication process. However, one of the main disadvantages is the necessity to contact the a-Si:H films by a Transparent Conductive Oxide (TCO) film in order to get low contact resistances and good optical properties. Typically, Indium Tin Oxide (ITO) is used as contact material, but a big effort is being paid to find cheaper materials like Boron or Aluminum-doped Zinc Oxides [5-6].

Recently, an alternative based on laser processing has been proposed to create highly-doped regions into c-Si with low thermal budget. Dielectric layers deposited at low temperature can be used as dopant sources with the advantage that they can simultaneously work as c-Si passivation layers and reduce optical reflectance. Additionally, an electrostatically induced emitter based on the fixed charge density at the dielectric/c-Si interface is created between the laser-processed regions. The concept of induced emitters was already proposed in the 80's [7], concluding that the distance between contacts must be short (in the range of hundreds of microns) to keep ohmic losses under control [8]. As a consequence, these structures must be located at the rear side of the cell where all the laser processed regions can be contacted by a continuous metallic film without increasing shadowing losses [9]. Recently, an efficiency of 18.1 % has been reported for n-type c-Si solar cells with a rear $p^+$ emitter based on laser processed $Al_2O_3$ films [10].

In this work, we focus on the performance of n-type c-Si solar cells whose emitters are formed by laser processing $Al_2O_3/SiC_x$ stacks. This type of emitters has been already applied to the Doped by Laser (DopLa) cell concept where all the highly-doped regions are created by laser processing dielectric films [11]. In particular, we combined the $p^+$ emitters at the rear side with a laser processed phosphorus-doped silicon carbide film ($SiC_x$(n)) at the front surface to form the base contacts. These contacts were separated 1 mm, which was the distance between front fingers, resulting in a device performance limited by ohmic losses due to the relatively long distance between them. As a consequence, the potential of the laser processed emitter could not be fully extracted in the final device. In order to overcome this limitation, in this work we replace the base contact at the front surface by a typical HIT structure, i.e. a stack of ITO/a-Si:H(n)/a-Si:H(i). We also fabricated solar cells with a HIT emitter on the rear surface and identical front surface configuration. Figure 1 shows the cross-sections of the fabricated devices labeled as Doped by Laser emitter (DopLa-Emitter) and Rear Emitter-HIT (RE-HIT) for a direct comparison of emitter performance in finished devices.

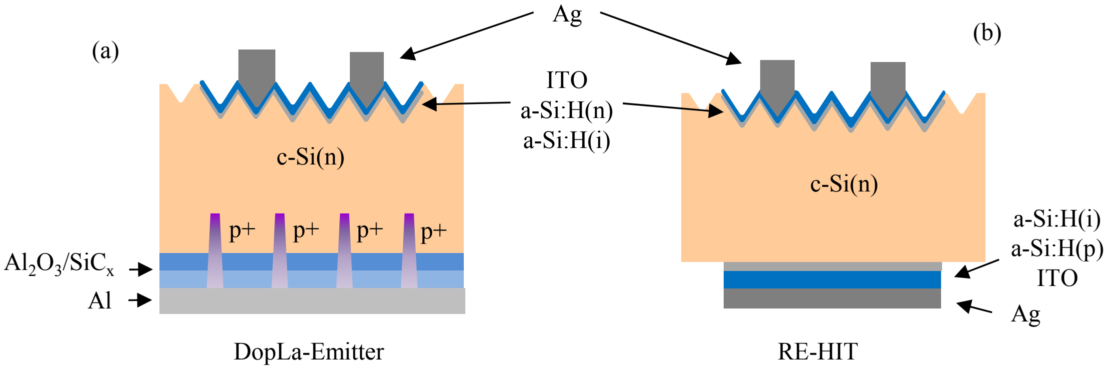


Fig.1 (a) DopLa-Emitter cell structure; (b) RE-HIT cell structure

## 2. Experimental

We used 260 μm-thick 1.4 Ωcm FZ c-Si wafers as substrates for solar cell fabrication that were textured at the front surface. In the case of DopLa-Emitter structures, we symmetrically deposited a 50 nm-thick $Al_2O_3$ film by Atomic Layer Deposition using Tri-Methyl Aluminum (TMA) and water as gas precursors. Next, these samples were annealed at 375 ºC for 20 minutes to activate the fixed charge density located at the $Al_2O_3$/c-Si interface. At the rear side, we capped the $Al_2O_3$ film by a 50 nm-thick dielectric silicon carbide ($SiC_x$) deposited by Plasma Enhanced Chemical Vapor Deposition (PECVD). This layer is close to stoichiometric composition (refractive index of 2.0 at 633 nm) and transparent to photons with $\lambda > 500$ nm (see reference [12] for a detailed description of the optical properties of the resulting film stack). On the front surface, we etched the $Al_2O_3$ film by diluted HF and deposited by PECVD a a-Si:H(i)/a-Si:H(n) stack followed by the deposition of a 75 nm-thick ITO film. The point-like $p^+$ regions of the rear emitter were defined in an hexagonal matrix using a Q-switched Nd:YAG laser (StarMark SMP 100II Rofin-Baasel) emitting at 1064 nm in TEM00. We used a laser power of 0.9 W leading to spots on the film stack with a diameter of about 50 μm. This laser process simultaneously ablates the dielectric and melts the c-Si allowing the diffusion of Aluminum atoms located at the $Al_2O_3$ film [13]. We fabricated solar cells with distances between laser spots or *pitch* ranging from 200 to 350 μm with an area of 1x1 $cm^2$. Finally, the rear emitter is contacted by 1 μm thick Aluminum film while at the front contact we defined a metal grid on the ITO by evaporating about 3μm-thick silver layer through a shadowing mask.

Regarding the RE-HIT, we started with a complete RCA cleaning step and the deposition of the a-Si:H(i)/a-Si:H(p) stack at the rear surface followed by a-Si:H(i)/a-Si:H(n) deposition on the front side, all by PECVD. Next, we deposited optimized ITO films on both front and the rear surfaces. In order to delimit the device area, at the rear surface we defined 1x1 $cm^2$ squares on the ITO followed by $CF_4$+$O_2$ plasma etching of the amorphous silicon emitter left in-between. Finally, the rear emitter was contacted by 0.5 μm-thick silver while on the front surface we defined identical metal grid of silver than in the previous devices. As a consequence, we obtained RE-HIT and DopLa-Emitter devices whose only difference is the emitter configuration.

## 3. Results and discussion

Firstly, we characterized both emitters by measuring the corresponding $J_{oe}$ from lifetime measurements using the method proposed by Kane and Swanson [14]. In this method, the $J_{oe}$ is obtained from the slope of the $1/\tau_{eff}$ vs. $\Delta n$ at high injection once the rest of recombination mechanisms are subtracted. We prepared symmetrical samples with the RE-HIT emitter including the ITO deposition. In this case, only bulk intrinsic recombination, that includes radiative and Auger recombination modeled following ref. [15] are considered for the $J_{oe}$ calculation. For DopLa-Emitter, we symmetrically deposited the $Al_2O_3$/$SiC_x$ stack and only one face was laser processed with four different pitches: 200, 250, 300 and 350 μm. In this case, the recombination at the other surface is also subtracted (an effective surface recombination velocity of 3 cm/s is deduced for this passivated surface). Results for DopLa-Emitters are shown in figure 2,(a) together with the best linear fit of the experimental data. The obtained $J_{oe}$ values are 30, 43, 59 and 103 fA/$cm^2$ for pitch decreasing from 350 to 200 μm. As a first approach, we can assign all the recombination to the laser processed spots. As a consequence, $J_{oe}$ values would linearly increase with the density of $p^+$ regions. As it can be seen in the inset of figure 2,(a), a linear behavior is observed for the three lower $J_{oe}$ values, i.e. for longer pitches. From the slope of the linear fit we can calculate a $J_{oe}$ value per spot of 1.65 pA/$cm^2$, assuming a laser spot with a diameter of 50 μm. This linear trend is lost for the 200 μm pitch sample that shows a $J_{oe}$ higher than expected. This increase in recombination could be attributed to damaged regions in the spot surroundings that are big enough to be connected for such a short pitch jeopardizing the passivation of the whole surface. For example, evidences of surface passivation losses up to 100 μm far away from the laser spot have been obtained by micro-scale characterization [16]. On the other hand, for RE-HIT we obtained a lower value of 34 fA/$cm^2$ (not shown in the graph). From these lifetime data, we conclude that for similar recombination activity in both emitters, long pitches in the range of 300-350 μm would be necessary for the DopLa-Emitter. However, this first guess about optimum pitch lacks information about carrier transport, since the measurement is done under open-circuit conditions. Moreover, additional recombination will arise in metallized devices, as it will be shown below. For these reasons, in the rest of the paper we focus on characterizing these emitters in finished devices under more realistic conditions, paying special attention to *FF* and $J_{0e}$.

We fabricated solar cells including these emitters as explained in the experimental section. For these devices, we measured $\tau_{eff}$ vs. $\Delta n$ dependence in cell precursors after finishing the corresponding film deposition on both surfaces but before metallization. Notice that in RE-HIT devices the emitter is already created while for DopLa-Emitter samples the rear surface is just covered with dielectric films and the laser process is needed to form the emitter. In figure 2,(b) we plot the measured data for those cell precursors. For the case of DopLa-Emitter samples we also plot the results after laser processing the emitter with a pitch of 250 µm. As it can be seen, before laser processing the recombination is similar in both emitters while lifetime significantly decreases after it. This result indicates that recombination in the laser processed $p^+$ regions is dominant in DopLa-Emitter solar cells and, what is more important, the quality of front surface passivation is good enough to see the impact of emitter performance on solar cell results.

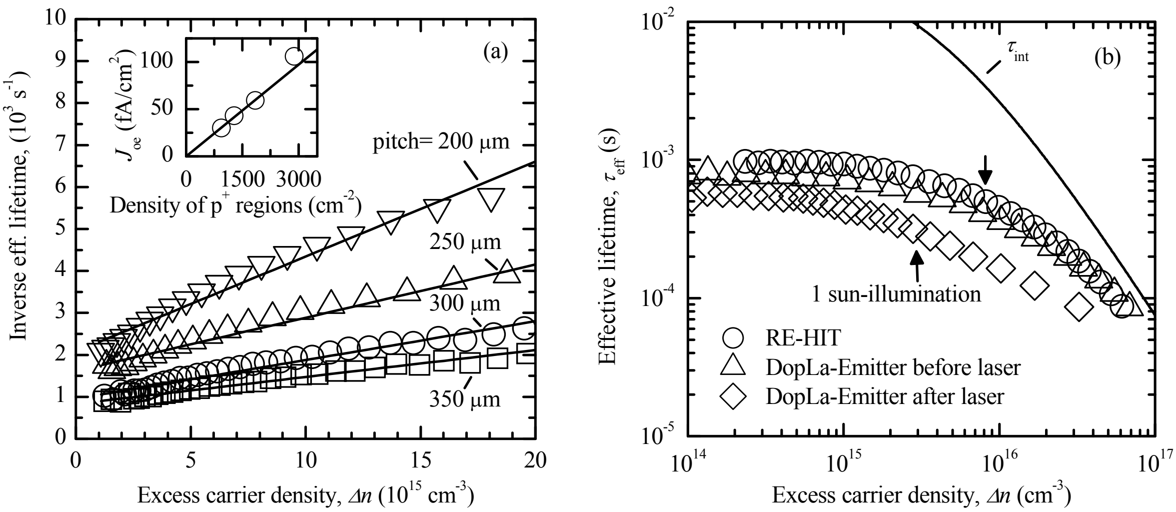


Fig. 2.(a) $1/\tau_{eff}$ vs. $\Delta n$ for $J_{oe}$ extraction. The obtained Joe values are 30, 43, 59 and 103 fA/cm$^2$ for pitches of 350, 300, 250 and 200 µm respectively; inset: $J_{oe}$ values vs. density of $p^+$ regions where a linear trend is observed for long pitches. (b) $\tau_{eff}$ vs. $\Delta n$ for solar cell precursors. The laser processing consisted of the creation of $p^+$ regions with a pitch of 250 µm.

Table 1. Photovoltaic figures of 1x1 cm$^2$ DopLa-Emitter cells with different rear pitch and RE-HIT cells.

| Pitch (µm) | $J_{sc}$ (mA/cm$^2$) | $V_{oc}$ (mV) | *FF* (%) | $\eta$ (%) |
|---|---|---|---|---|
| 200 | 37.5 | 625 | 75.4 | 17.7 |
| 250 | 37.6 | 647 | 74.3 | 18.1 |
| 300 | 37.7 | 650 | 72.6 | 17.8 |
| 350 | 37.1 | 658 | 70.4 | 17.2 |
| RE-HIT | 37.7 | 666 | 75.7 | 19.0 |

In Table 1 we show the photovoltaic figures measured under standard conditions (25 ºC, AM1.5g, 100 mW/cm$^2$) of the finished devices. Focusing on DopLa-Emitter samples, the results are much better than the ones reported in reference [11] where solar cells with these emitters were fabricated. In that work, the main limitation of those devices was the poor passivation of the front side (best $V_{oc}$ was 627 mV) and the ohmic losses introduced by point-like base contacts (best *FF* with 200 µm pitch was 69.8 %). These problems have been overcome with the introduction of the front contact based on silicon heterojunction technology. Now, best FF is 75.4 % similar to the one obtained for RE-HIT solar cells indicating that the ohmic losses introduced by the 200 µm pitch emitter are in the same range than the heterojunction emitter. As expected, *FF* decreases with pitch due to the high sheet resistance of the induced emitter in between $p^+$ regions [10-11]. On the other hand, $V_{oc}$ is clearly impacted by the emitter pitch confirming that the recombination in the laser processed $p^+$ regions are prevailing in the device performance. As a consequence of the trade-off between $V_{oc}$ and $FF$, best efficiency is obtained for 250 µm pitch sample with 18.1 %. Comparing DopLa-Emitter and RE-HIT devices we observe a better $V_{oc}$ value for the latter which is attributed to a lower recombination in the HIT emitter, as suggested from the lifetime data of cell precursors.

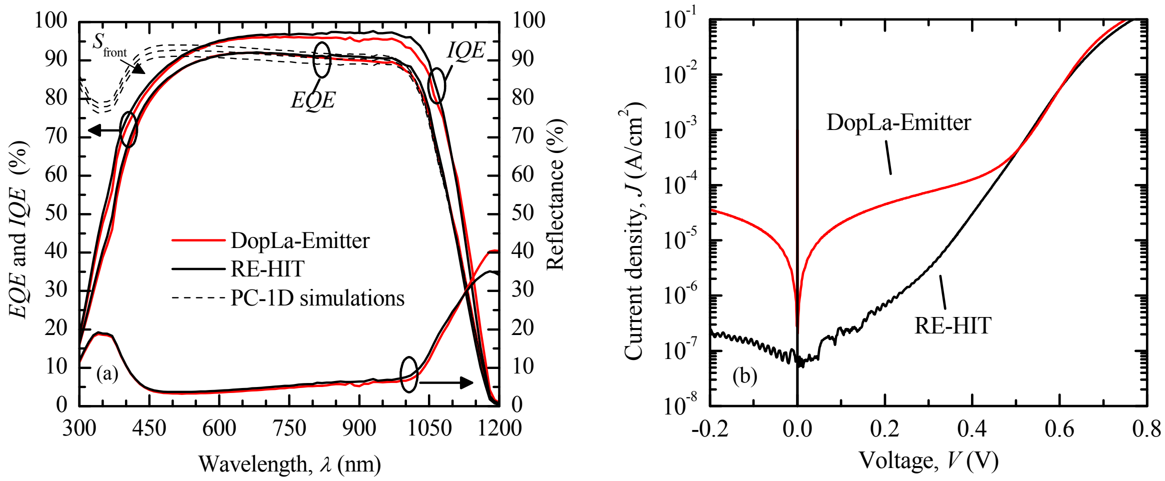


Fig. 3.(a) EQE, IQE and Reflectance of RE-HIT and 250 µm pitch DopLa-Emitter solar cells. Additionally, PC-1D simulations of simple rear emitter device are shown with $S_{front}$ ranging from 10 to 25 cm/s. (b) Dark J-V curves of RE-HIT and a typical DopLa-Emitter device.

As a further device characterization, we measured External Quantum Efficiency (*EQE*) and device reflectance (*R*). From these values we calculate Internal Quantum Efficiency (*IQE*) as $IQE = EQE/(1-R)$. All these magnitudes for RE-HIT cell and 250 µm pitch DopLa-Emitter cell are shown in figure 3,(a). As it can be seen, front reflectance is almost identical except for $\lambda$ beyond 1100 nm where the DopLa-Emitter device shows higher values indicating a better back reflector. The advantage of $Al_2O_3/SiC_x$ dielectric stack is probably based on its transparency for the photons that reach the rear surface compared to ITO/a-Si:H combination. Despite this feature is not relevant to the devices presented hereby, this advantage of DopLa-Emitter could be important if thinner c-Si substrates are used. Focusing on EQE, it is similar in both devices, as expected from the $J_{sc}$ values, while IQE is slightly better for RE-HIT device in the 750-1050 nm range. This difference could be attributed to the lower recombination of the emitter located at the rear surface.

Finally, we are interested in calculating $J_{0e}$ for the fabricated devices. Due to the location of the emitter at the rear side, the EQE level is strongly impacted by the surface recombination velocity at the front side ($S_{front}$). To get this value, we use PC-1D simulations that reproduce the main device features (thickness, substrate doping density and experimental reflectance) with a simple back junction configuration. As it can be seen in figure 3,(b), simulations (dashed lines) reproduce quite well the experimental data except for wavelengths below 600 nm. This difference is related to the light absorption in the amorphous silicon films deposited on top of the device not included in the PC-1D simulations. To demonstrate the accuracy in the determination of $S_{front}$, we show in figure 3,(a) simulations with $S_{front}$ values of 10, 17 and 25 cm/s. By fitting the experimental curves for all the samples, we estimate a $S_{front}$ in the range of 17±2 cm/s. With this value we are able to calculate the base component of saturation current density of the solar cells ($J_{0b}$) applying the classical semiconductor theory [17]:

$$J_{0b} = q\frac{n_i^2}{N_D}\frac{D_p}{L_{eff}} \quad (1) \qquad \text{with} \qquad L_{eff} = L\left(\frac{1+\dfrac{S_{front}L}{D_p}\tanh\left(\dfrac{w}{L}\right)}{\dfrac{S_{front}L}{D_p}+\tanh\left(\dfrac{w}{L}\right)}\right) \quad (2)$$

where symbols have their usual meaning. Assuming that $L$ is infinity (no recombination in the bulk) and using $D_p$ = 11.77 cm$^2$/s, we obtain a $J_{0b}$ of 55±7 fA/cm$^2$. Now, we can calculate the total saturation current density of the solar cells by applying the superposition principle between illuminated and dark responses. In other words, we apply that $J_0 = J_{sc} \times \exp(-V_{oc}/v_t)$. Once we have $J_0$, we can calculate $J_{0e}$ by subtracting the base term calculated above. It must be mentioned that by this approach we neglect high-injection effects that could appear due to the relatively low donor density of the substrate and could slightly modify the obtained $J_{0e}$ values. Despite these inaccuracies, we think that the $J_{0e}$ values calculated in this way are still a good reference to compare the recombination properties in finished devices of the emitters studied hereby. The resulting values are shown in Table 2.

Table 2. Estimated $J_{0e}$ values of DopLa-Emitter cells with different rear pitch and RE-HIT cells.

| Pitch (μm) | $J_0$ (fA/cm$^2$) | $J_{0b}$ (fA/cm$^2$) | $J_{0e}$ (fA/cm$^2$) |
|---|---|---|---|
| 200 | 1.029 | 55±7 | 964±7 |
| 250 | 434 | 55±7 | 379±7 |
| 300 | 387 | 55±7 | 332±7 |
| 350 | 279 | 55±7 | 224±7 |
| RE-HIT | 208 | 55±7 | 153±7 |

As it can be seen, the obtained values have the same tendency than in the experiment where $J_{0e}$ was determined from lifetime measurements presented above, but with much higher values. For RE-HIT devices, we think that device perimeter is playing and important role in increasing emitter recombination. A plasma etching is used to define 1x1 cm$^2$ emitter regions introducing an additional recombination not present in lifetime samples. For DopLa-Emitter samples, our opinion is that the additional recombination comes from the laser spot perimeter where the p$^+$ regions are less doped. In reference [18], a study of the dopant distribution in the laser spots defined onto $Al_2O_3$ films is reported leading to the conclusion that not all the spot is fully diffused. In lifetime samples, c-Si surface at the laser spots is bare and some degree of surface passivation is provided by the native oxide. On the contrary, after metallization all the surface is active for recombination. This is particularly critical for electrically transparent emitters, i.e. low-doped regions. For the laser power used in the solar cells, these regions are located at the spot perimeter [18]. Additionally, an increase in the leakage current of the diodes would be expected since the p$^+$/n junction can not be adequately accommodated (the low doped p$^+$ emitter can be carrier depleted or the metal can directly shunt the shallow p$^+$ region). This is confirmed in the dark $J$-$V$ curves shown in figure 3,(b) where DopLa-Emitter devices typically have a much higher current density at low voltages than RE-HIT ones.

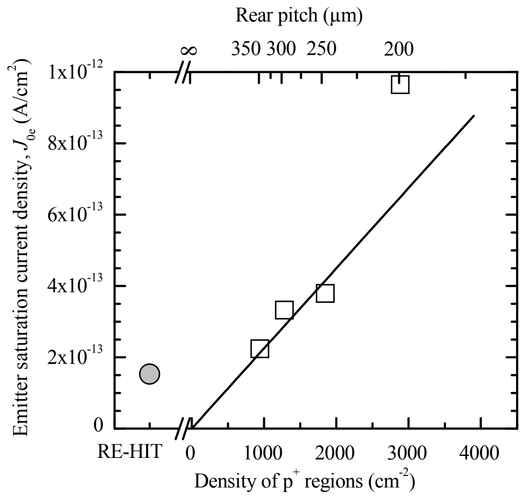


Fig. 4. $J_{oe}$ vs. density of p$^+$ regions for the fabricated DopLa-Emitter devices. The Joe value of RE-HIT devices is also shown for direct comparison. Again, a linear trend is observed for long pitches while the 200 μm pitch sample has an additional recombination.

Interestingly, we can estimate the $J_{0e}$ introduced by each point-like $p^+$ region in the final device using the same approach than the one used for lifetime samples in figure 1. We plot $J_{0e}$ vs. density of $p^+$ regions for DopLa-Emitters deduced from the finished devices in figure 4. Additionally, the $J_{0e}$ of the RE-HIT sample is also plotted for direct comparison. As it can be seen, $J_{0e}$ linearly increases for shorter pitches while for the highest explored density of $p^+$ regions, i.e. the shortest pitch, a much higher $J_{0e}$ is obtained. This effect was already identified in the lifetime experiment and it is attributed to a damaged surface passivation in the regions in between laser spots. Discarding this last point, a linear fit of the $J_{0e}$ vs. density of $p^+$ regions gives a $J_{0e}$ per spot of 11.46 pA/cm$^2$ (assuming a laser spot with a diameter of 50 μm). This result represents more accurately the quality of the $p^+$ regions and underlines the coarse characteristic of our laser doping technique compared to conventional diffusion. Although further efforts will be paid to explore less thermal processes reducing laser wavelength and/or pulse length, in our opinion laser processed area fractions in the 1-5 % range will be necessary to keep recombination under control introducing additional ohmic losses. Although this trade-off would probably prevent DopLa-Emitter to be an ultra high-efficiency feature like HIT emitters, noteworthy efficiencies, as the ones presented in this work, are still reachable and it could be considered a feasible alternative for cost-effective low temperature emitters.

## 4. Conclusions

In this work, we have studied the performance of emitters based on laser processed $Al_2O_3/SiC_x$ films. From lifetime measurements, similar recombination activity is measured for DopLa-Emitter with pitches in the 300-350 μm range compared to RE-HIT emitter. For very short pitches (200 μm), additional recombination is observed probably due to damaged regions in the vicinity of laser spots. In finished devices, a trade-off between $FF$ and $V_{oc}$ is observed leading to a maximum efficiency of 18.1 % with 250 μm rear pitch. From reflectance measurements, a better back reflector properties are measured for DopLa-Emitter solar cells while a significant increase in $J_{0e}$ is deduced in finished devices. The responsible of this poor performance is an additional recombination in the laser spots not seen in lifetime samples. The low doping density at spot perimeter leads to electrically transparent regions that increase recombination once their surface is metallized. Despite the higher recombination and additional ohmic losses, significant efficiencies are reached demonstrating that DopLa-Emitters can be considered a cost-effective structure.

## Acknowledgements

This work has been supported by the Spanish Government under project TEC 2011-26329 and by the European Union's Seventh Framework Programme for research, technological development and demonstration under project HERCULES (Grant agreement:608498).

## References

[1] Taguchi M, Yano A, Tohoda S, Matsuyama K, Nakamura Y, Nishiwaki T, Fujita K, Maruyama E; 24.7% Record Efficiency HIT Solar Cell on Thin Silicon Wafer. IEEE Journal of Photovoltaics 2014; 4(1): 96–99.

[2] Tsunomaru Y, Yoshimine Y, Taguchi M, Baba T, Kinoshita T, Kanno H, Sakata H, Maruyama E, Tanaka M; Twenty-two percent efficiency HIT Solar Cell. Solar Energy Materials and Solar Cells 2009; 93(6): 670–673.

[3] Masuko K, Shigematsu M, Hashiguchi T, Fujishima D, Kai M, Yoshimura N, Yamaguchi T, Ichihashi Y, Mishima T, Matsubara N, Yamanishi T, Takahama T, Taguchi M, Maruyama E, Okamoto S. Achievement of more than 25% conversion efficiency with crystalline silicon heterojunction solar cell. IEEE Journal of Photovoltaics 2014; 4: 1433-5.

[4] Nakamura J, Asano N, Hieda T, Okamoto C, Katayama H, Nakamura K. Development of Hetero-Junction Back Contact Si Solar Cells. IEEE Journal of Photovoltaics 2014; 4: 1491-5.

[5] Ruske F, Roczen M, Lee K, Wimmer M, Gall S, Hüpkes J, Hrunski D, Rech B. Improved electrical transport in Al-doped zinc oxide by thermal treatment. Journal of Applied Physics 2010; 107: 013708.

[6] Favier A, Muñoz D, Martín de Nicolás S, Ribeyron PJ. Boron-doped zinc oxide layers grown by metal-organic CVD for silicon heterojunction solar cells applications. Solar Energy Materials and Solar Cells 2011; 95: 1057.

[7] Hezel R, Schoerner R. Plasma Si nitride-A promising dielectric to achieve high-quality silicon MIS/IL solar cells. Journal of Applied Physics 1981; 52: 3076.

[8] Kuhlmann B, Aberle AG, Hezel R, Heiser G, Simulation and optimization of metal-insulator-semiconductor inversion-layer silicon solar cells. IEEE Transactions on Electron Devices 2000; 47: 2167.
[9] Martín I, Lövblom R, Alcubilla R; High-efficiency solar cells based on inversion layer emitters, In: Proceedings of 24th EUPVSEC, Hamburg, Germany, 2009, pp. 1985-1991.
[10] Werner F, Larionova Y, Zielke D, Ohrdes T, Schmidt J. Aluminum-oxide-based inversion layer solar cells on n-type crystalline silicon: Fundamental properties and efficiency potential. Journal of Applied Physics 2014; 115: 073702.
[11] Martín I, Colina M, Coll A, López G, Ortega P, Orpella A, Alcubilla R. c-Si Solar Cells based on Laser-processed Dielectric Films. Energy Procedia 2014; 55: 255 – 264.
[12] López G, Ortega P, Voz C, Martín I, Colina M, Morales AB, Orpella A, Alcubilla R. Surface passivation and optical characterization of Al2O3/a-SiCx stacks on c-Si substrates. Beilstein Journal of Nanotechnology 2013; 4: 726.
[13] Martín I, Ortega P, Colina M, Orpella A, López G, Alcubilla R. Laser processing of $Al_2O_3$/a-$SiC_x$:H stacks: a feasible solution for the rear surface of high-efficiency p-type c-Si solar cells. Progress in Photovoltaics: Research and Applications 2013; 21: 1171-1175.
[14] Kane DE, Swanson RM. Measurement of the emitter saturation current by a contactless photoconductivity decay method. In: Proceedings of IEEE 18th Photovoltaic Specialist Conference, Las Vegas, USA, 1985; 578.
[15] Kerr MJ, Cuevas A. General parameterization of Auger recombination in crystalline silicon. Journal of Applied Physics 2002; 91: 2473.
[16] Roigé A, Ossó JO, Martín I, Voz C, Ortega P, Alcubilla R, Vega LF. Micro-scale characterization of surface recombination at the vicinity of laser fired contacts. Submitted to IEEE Journal of Photovoltaics.
[17] Sze S, Lee MK. Semiconductor devices: physics and technology. Singapore: John Wiley & Sons; 2013.
[18] Roigé A, Alvarez J, Kleider JP, Martín I, Alcubilla R, Vega LF. Microscale Spatially Resolved Characterization of Highly Doped Regions in Laser-Fired Contacts for High-Efficiency Crystalline Si Solar Cells. IEEE Journal of Photovoltaics 2015; 5: 545.